NUCLEAR REACTIONS

- $A + a \rightarrow B + b + Q$ or $A(a, b)B$

  $Q > 0$ EXOTHERMIC

  $Q < 0$ ENDOTHERMIC

- Nucleosynthesis may involve

  A = nuclide with

  a = electrons

  protons, other nuclides

  photons

  neutrons

  neutrinos

TABLE 1

Reduced de Broglie wavelengths for various particles and energies

Energy (MeV)	Wavelength (fm)				
	Photon	Electron	Proton	α-Particle	^{16}O
0.1	2000.	589	14.5	7.2	3.61
1.	200	140	4.6	2.3	1.14
10	20.	18.7	1.4	0.72	0.36
100	2.0	2.0	0.45	0.23	0.11
1000	0.2	0.2	0.12	0.068	0.035

CROSS-SECTIONS & RATE CONSTANTS

In general, $\sigma = \sigma(v)$

$$\text{Rate} = n_A n_B \int_0^\infty \phi(v)\,\sigma(v)\,v\,dv$$

$$= \frac{n_A n_B}{(1+\delta_{AB})} \langle \sigma v \rangle$$

$cm^{-3} s^{-1}$ $cm^{3} s^{-1}$

ASSUME MAXWELLIAN VELOCITY DIST'N

$$\phi(v)\,dv = 4\pi v^2 \left(\frac{m}{2\pi kT}\right)^{3/2} \exp\left(-\frac{mv^2}{2kT}\right) dv$$

for non-degenerate gas

For $A + B \rightarrow C + D$, velocity distribution needed is the relative velocity distribution

$m \rightarrow \mu =$ reduced mass

$$\frac{1}{\mu} = \frac{1}{m_A} + \frac{1}{m_B}$$

$$\mu = \frac{m_A m_B}{m_A + m_B}$$

$$\langle \sigma v \rangle = 4\pi \left(\frac{\mu}{2\pi kT} \right)^{3/2} \int_0^\infty v^3 \sigma(v) \exp\left(-\frac{\mu v^2}{2kT} \right) dv$$

$$= \left(\frac{8}{\pi \mu} \right)^{1/2} \frac{1}{(kT)^{3/2}} \int_0^\infty \sigma(E) E \exp\left(-\frac{E}{kT} \right) dE$$

EXOTHERMIC $\sigma(E) =$ finite at $E = 0$

ENDOTHERMIC $\sigma(E) = 0$ for $E \leq -Q$

UNITS – once again!

- STELLAR MODELS often give total density (ρ) and mass fractions

- $n_i = \dfrac{\rho_i}{A_i m_u} = N_A \dfrac{\rho_i}{A_i}$

  where $N_A = 1/m_u = 6.02214 \times 10^{23}$ mole^{-1}

  = AVOGADRO's NUMBER

- With $X_i = \rho_i / \rho$

  Rate $R = \dfrac{\rho X_A}{A_A} \cdot \dfrac{\rho X_B}{A_B} N_A^2 \dfrac{\langle \sigma v \rangle}{(1+\delta_{AB})}$

  $= \rho^2 N_A^2 Y_A Y_B \langle \sigma v \rangle / (1+\delta_{AB})$

  where $Y_i = \dfrac{X_i}{A_i}$ is mole fraction of i

RATE CONSTANTS often in $cm^3 s^{-1} mole^{-1}$ then

$[\sigma v]$ in $cm^3 s^{-1} mole^{-1}$

$= N_A \langle \sigma v \rangle$ in $cm^3 s^{-1}$

and

$$R\ [cm^{-3} s^{-1}] = \frac{\rho^2 N_A Y_A Y_B}{(1+\delta_{AB})} [\sigma v]$$

ORDER OF MAGNITUDE ESTIMATES FOR σ

If hard spheres,

$$\sigma = \pi (R_A + R_B)^2$$

$$\simeq 1 \text{ barn}$$

BUT

i) Nuclei are not hard spheres
   – see Table of de Br wavelengths

ii) Coulomb barrier penetration

(Rolfs Fig 4.2)

$$E_{barrier} \sim \frac{Z_A Z_B e^2}{(R_A + R_B)}$$

$$\sim \frac{Z_A Z_B}{A_A^{1/3} + A_B^{1/3}} \text{ in MeV}$$

$$\cong 6 \times 10^9 K \text{ for } p+p$$

but $T_\odot$ (core) $\sim 10^7 K$

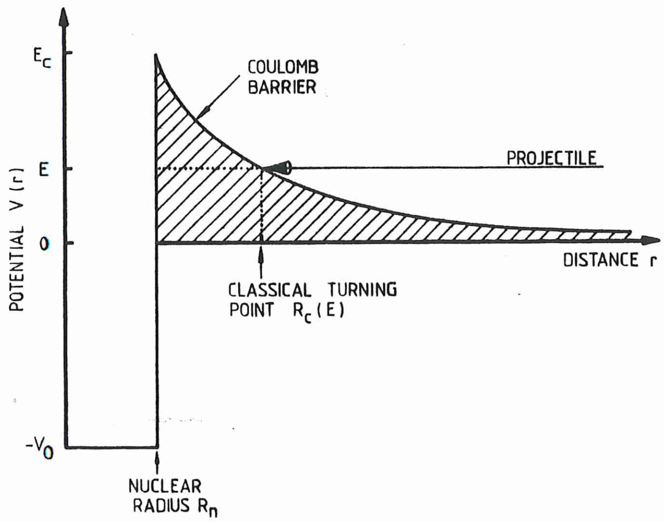

FIGURE 4.2. Schematic representation of the combined nuclear and Coulomb potentials. A projectile incident with energy $E < E_C$ has to penetrate the Coulomb barrier in order to reach the nuclear domain. Classically, the projectile would reach the closest distance to the nucleus at the turning point R_c.

For $E \ll E_{BARRIER}$, tunnelling probability is

$$P = \exp(-2\pi\eta) = \exp\left[-\left(\frac{E_G}{E}\right)^{1/2}\right]$$

Sommerfeld parameter

Gamow energy

where $E_G = 0.979\, Z_A^2 Z_B^2 \mu$ [MeV]

→ usually only particles in tail of M-B distribution are effective

Rolfs 4.6
Boo 7.3
Ilia Fig 3.13 p167

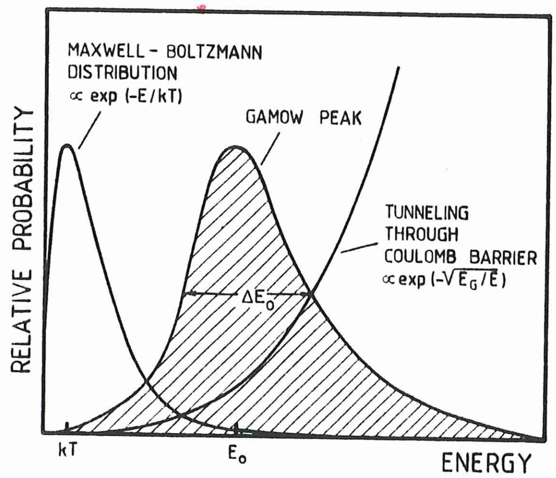

FIGURE 4.6. The dominant energy-dependent functions are shown for nuclear reactions between charged particles. While both the energy distribution function (Maxwell-Boltzmann) and the quantum mechanical tunneling function through the Coulomb barrier are small for the overlap region, the convolution of the two functions results in a peak (the Gamow peak) near the energy E_0, giving a sufficiently high probability to allow a significant number of reactions to occur. The energy of the Gamow peak is generally much larger than kT.

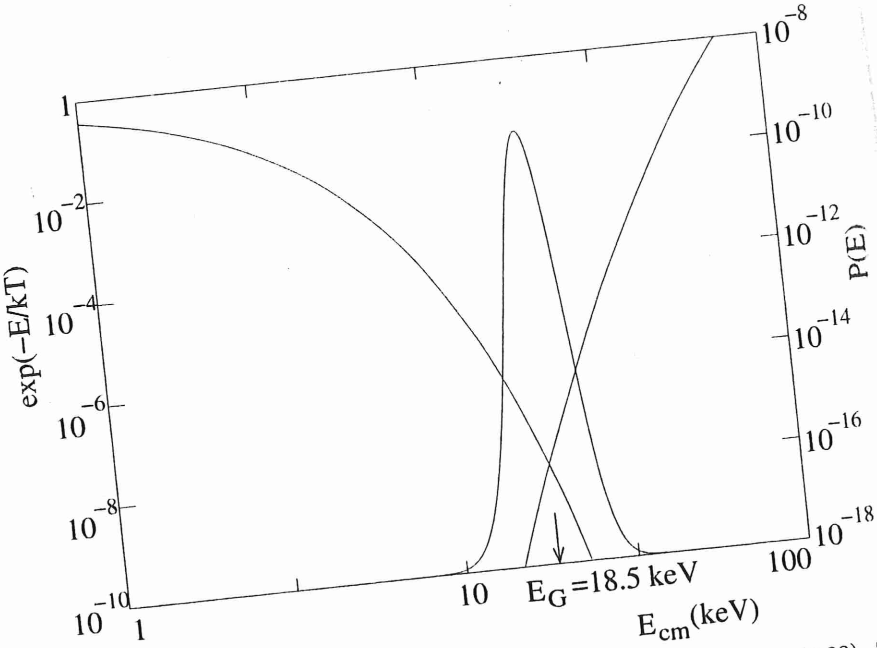

Fig. 7.3. Factors entering the calculation of the pair reaction rate (7.22). The Boltzmann factor $\exp(-E/kT)$ (logarithmic scale on the left) and the barrier penetration probability $P(E) = \exp(-\sqrt{E_B/E})$ (7.13) (logarithmic scale on the right) are calculated for $kT = 1\,\mathrm{keV}$ (corresponding to the center of the Sun) and for the reaction $^3\mathrm{He}\ ^3\mathrm{He} \rightarrow\ ^4\mathrm{He}\,pp$. The product is the Gaussian-like curve in the center (shown on a linear scale). It is maximized at $E_G = (\sqrt{E_B}kT/2)^{2/3} \sim 18.5\,\mathrm{keV}$ and most reactions occur within $\sim 5\,\mathrm{keV}$ of this value. Note the small values of $\exp(-E_{Gm}/kT) \sim 10^{-8}$ and $P(E_G) \sim 10^{-16}$.

iii) The nature of the force controlling the short-range interaction

- Strong nuclear force: $^{15}N(p,\alpha)^{12}C$ $\sigma \sim 0.5\,b$
- EM force: $^{3}He(\alpha,\gamma)^{7}Be$ $\sigma \sim 10^{-6}\,b$
- Weak force $p(p, e^{+}\nu_e)d$ $\sigma \sim 10^{-20}\,b$

for CoMass $E \sim 2\,MeV$

i.e., ~ height of Coulomb barrier.

ONLY Strong nuclear force has $\sigma \sim$ geometric σ.

THE ASTROPHYSICAL S-FACTOR

- Convenient for extrapolation and demonstration of details in σ

$$\sigma(E) \approx \frac{1}{E} \exp\left[-\left(\frac{E_G}{E}\right)^{1/2}\right] S(E)$$

$\propto \lambda\!\!\!^{-2}$

Penetration term

$$\langle \sigma v \rangle = \left(\frac{8}{\pi \mu}\right)^{1/2} \frac{1}{(kT)^{3/2}} \int_0^\infty S(E) \exp\left[-\frac{E}{kT} - \left(\frac{E_G}{E}\right)^{1/2}\right] dE$$

Fig 4.4 | Rolfs

- extrapolation to lower E_{cm} "seems" safe!

VALUE OF S(E)

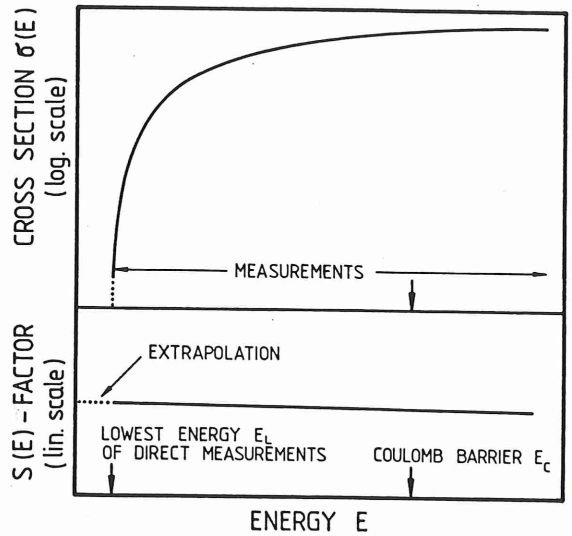

FIGURE 4.3. Cross section $\sigma(E)$ of a charged-particle–induced nuclear reaction drops sharply with decreasing energy E (by many orders of magnitude) for beam energies below the Coulomb barrier E_C, thus effectively providing a lower limit E_L to the beam energy at which experimental measurements can be made. Extrapolation to lower energies is more reliable if one uses the $S(E)$ factor.

Figure CC

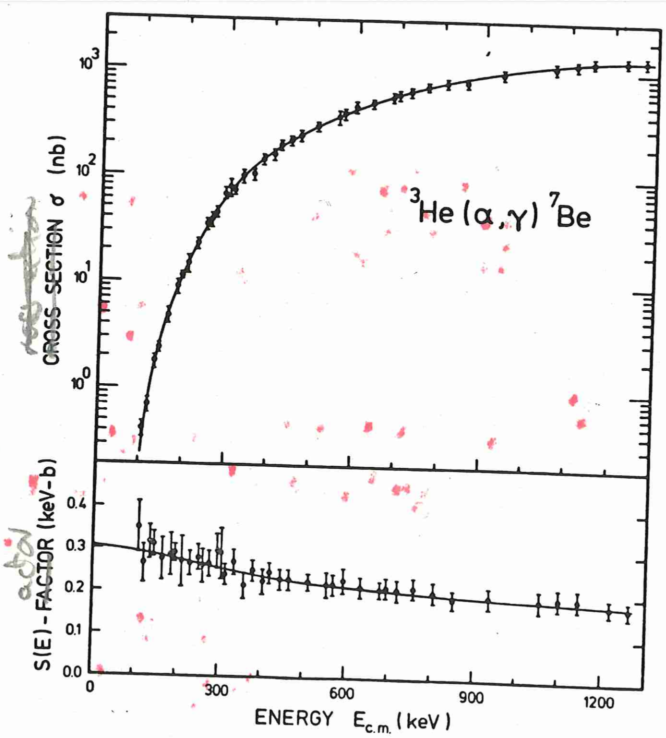

FIGURE 4.4. Energy dependence of the cross section $\sigma(E)$ and the factor $S(E)$ for the $^3He(\alpha, \gamma)^7Be$ reaction (Krä82). The line through the data points represents a theoretical description of the cross section in terms of the direct-capture model. This theory is used to extrapolate the data to zero energy. Data from other sources (chap. 6) give a higher absolute scale (40% difference).

The S-factor: an approximation

Replace $\exp\left[-\frac{E}{kT} - \left(\frac{E_G}{E}\right)^{1/2}\right]$ by the

Gaussian $\exp\left[-\left(\frac{E - E_0}{\Delta E_0/2}\right)^2\right]$

$$\exp\left[-\frac{E}{kT}-\left(\frac{E_G}{E}\right)^{1/2}\right] \cong I_{max}\exp\left[-\left(\frac{E-E_0}{\Delta E_0/2}\right)^2\right] \tag{1.18}$$

It may be readily shown (*Cauldrons*) that

$$E_0 = E_G^{1/3}\left(\frac{kT}{2}\right)^{2/3} = 1.220(Z_A^2 Z_B^2 \mu T_6^2)^{1/3} \tag{1.19}$$

$$\Delta E_0 = 4\left(\frac{E_0 kT}{3}\right)^{1/2} = 0.749(Z_A^2 Z_B^2 \mu T_6^5)^{1/6} \tag{1.20}$$

$$I_{max} = \exp\left(-\frac{3E_0}{kT}\right) \tag{1.21}$$

$$\tag{1.22}$$

where the numerical expressions give E_0 and ΔE_0 in keV. Note that $\Delta E_0/E_0 \sim (kT/E_0)^{1/2}$ and, since $E_0 \gg kT$ in many circumstances, ΔE_0 will be much smaller than E_0.

In this approximation, the rate constant (equation(1.17) is

$$< \sigma v >= \left(\frac{2}{\mu}\right)^{1/2}\frac{\Delta E_0}{(kT)^{3/2}}S_{eff}(E_0)\exp\left(-\frac{3E_0}{kT}\right) \tag{1.23}$$

where $S_{eff}(E_0)$ is the value of $S(E)$ at $E = \cancel{E(}E_0\cancel{)}$ in the event that $S(E)$ varies with energy; a steep energy dependence around E_0 would invalidate the assumption of a constant $S(E)$.

For numerical evaluation, it is helpful to introduce

$$\beta = \frac{3E_0}{kT} = 42.46\left(\frac{Z_A^2 Z_B^2 \mu}{T_6}\right)^{1/3} \tag{1.24}$$

and substitute in equation(1.23) to obtain

$$< \sigma v >= 7.20 \times 10^{-19}\frac{1}{\mu Z_A Z_B}\beta^2 S_{eff}(E_0)\exp(-\beta) \tag{1.25}$$

Equation (1.25) may be rewritten as

$$< \sigma v >= 1.301 \times 10^{-14}\left(\frac{Z_A Z_B}{\mu}\right)^{1/3}\frac{S(E_{eff})}{T_9^{2/3}}\exp\left[-4.2486\left(\frac{Z_A^2 Z_B^2 \mu}{T_9}\right)^{1/3}\right] \tag{1.26}$$

TABLE

Tunnelling the Coulomb barrier

Reaction	E_{bar} (MeV)	T_6 (K)	E_{Th} (keV)	E_0 (keV)	$\Delta E_0/2$ (keV)	n	E_0/E_{bar}	E^{low}_{lab} (keV)
p+p	0.6	15	1.3	5.9	3.2	4	0.01	....[a]
p+^{14}N	2.3	15	1.3	26.5	6.8	20	0.01	100 ~~0.25~~
α+^{12}C	3.4	15	1.3	56.	9.8	42	0.02	1000
		200	17.2	315.1	85.	18	0.09	1000
^{12}C+^{12}C	8.6	15	1.3	147.	16.	112	0.02	2200
		700	60.3	1900.	390.	31	0.22	2200
^{16}O+^{16}O	14.0	15	1.3	237.	20.	182	0.02	6700
		2000.	172.3	6200.	1200.	35	0.44	6700

[a] Cross-section is theoretically evaluated.

The temperature dependence

As long as the Gamow energy is considerably less than the height of the Coulomb barrier, there is a marked sensitivity of the rate constant to temperature. To quantify this sensitivity in a simple manner, I write the rate constant as follows

$$< \sigma v >_T = < \sigma v >_0 \left(\frac{T}{T_0}\right)^n \tag{1.27}$$

By equating the derivatives $dln < \sigma v > /dT$ of this and equation (1.23), it is easily shown that

$$n \simeq \frac{\frac{3E_0}{kT} - 2}{3} = \frac{\beta - 2}{3} \tag{1.28}$$

Representative examples

To illustrate several aspects of the preceding discussion, I select five reactions representative of hydrostatic burning in stars. Hydrogen burning is represented by the $p+p$ and $p + {}^{14}$N where the former is from the *pp*-chain and the latter from the CN-cycle. The $\alpha + {}^{12}$C reaction is a part of helium burning. The final two reactions, ^{12}C + ^{12}C and ^{16}O + ^{16}O, power the terminal phases of massive stars. For each reaction, I list in Table CB the Coulomb barrier (E_{bar}), the thermal energy ($E_{th} = kT$), the Gamow peak energy (E_0), the width ΔE_0, and n (rounded off to the nearest integer). This information is tabulated for all reactions for $T_6 = 15$ and for the non-hydrogen burning reactions also for a temperature more representative of the conditions in a massive star at the time these reactions are initiated. In addition, I give the ratio E_0/E_{bar} for the assumed conditions; the smaller the ratio the greater the sensitivity of the rate constant to temperature or the greater the exponent n. Finally, I give the low energy limit (E_{lab}^{low}) of laboratory measurements of the cross-section. Note that E_0/E_{bar} for carbon and oxygen burning at the temperatures achieved in massive stars exceeds the value for which the approximation used for the tunnelling probability is accurate.

A General expression

Rarely will the S-factor be strictly constant; for example, the S-factor shown in Figure CC increases steadily to low energies. In such cases, the S-factor may be written as

$$S(E) = S(0) + \dot{S}(0)E + \frac{1}{2}\ddot{S}(0)E^2 + ... \tag{1.29}$$

The rate constant is given by equation (1.26) with

$$
\begin{aligned}
S_{eff}(0) &= S(0)\left[1+\frac{5kT}{36E_0}+\frac{\dot{S}(0)}{S(0)}\left(E_0+\frac{35}{36}kT\right)\right.\\
&\left. + \frac{1}{2}\frac{\ddot{S}(0)}{S(0)}\left(E_0^2+\frac{89}{36}E_0kT\right)\right] \qquad (1.30)
\end{aligned}
$$

Compilations of rate constants for astrophysicists' use provide analytical approximations to the rate constants that may be incorporated in computer programmes. For example, Angulo et al. (1999) adopt the following form for $[\sigma v] = N_A < \sigma v >$ for exothermic reactions without resonances

$$[\sigma v] = \frac{C_1}{T_9^{3/2}} \exp\left(-\frac{C_0}{T_9^{1/3}}\right)\left[1+\sum_{i=1}^{N_{rate}} c_i T_9^i\right] \qquad (1.31)$$

and give the coefficient C_1, the order of the polynomial N_{rate} and coefficients c_i obtained from a fit to the recommended rate constants. The constant $C_0 = 4.2486(Z_A Z_B \mu)^{1/3}$ from equations (1.25) and (1.23). A similar expression applies to endothermic reactions with $C_0/T_9^{1/3}$replaced by $(C_0'/T_9^{1/3} - D_0/T_9)$ where C_0' is computed as C_0 but with the nuclear charges and reduced mass corresponding to the exit channel, and $D_0 = |Q|/k = 11.605|Q|$ with the Q-value in MeV.

1.2.5 The Contribution of Resonances

As discussed in Sec. ..., the cross-section may show a local increase at a given energy for a particular pair of reactants in the entrance channel. This is referred to as a resonance for which the cross-section may be represented by the Breit-Wigner formula for a single isolated resonance

$$\sigma_{BW}(E) = \pi \bar{\lambda}^2 \omega \frac{\Gamma_a \Gamma_b}{(E-E_R)^2 + \Gamma^2/4} \qquad (1.32)$$

where Γ_a and Γ_b are the partial widths that denote the probabilities for formation and decay respectively of the resonant energy level in the compound nucleus, Γ is the sum of the partial widths in the exit (decay) channel. , $\bar{\lambda}$ is the de Broglie wavelength, and ω is a statistical factor

$$\omega = \frac{(2J+1)}{(2J_p+1)(2J_t+1)}(1+\delta_{pt}) \qquad (1.33)$$

where J is the total angular momentum of the resonant energy level, and J_p and J_t are spins of the projectile and target nuclei respectively. Energies and widths are in the centre-of-mass system. Note that the entrance channel

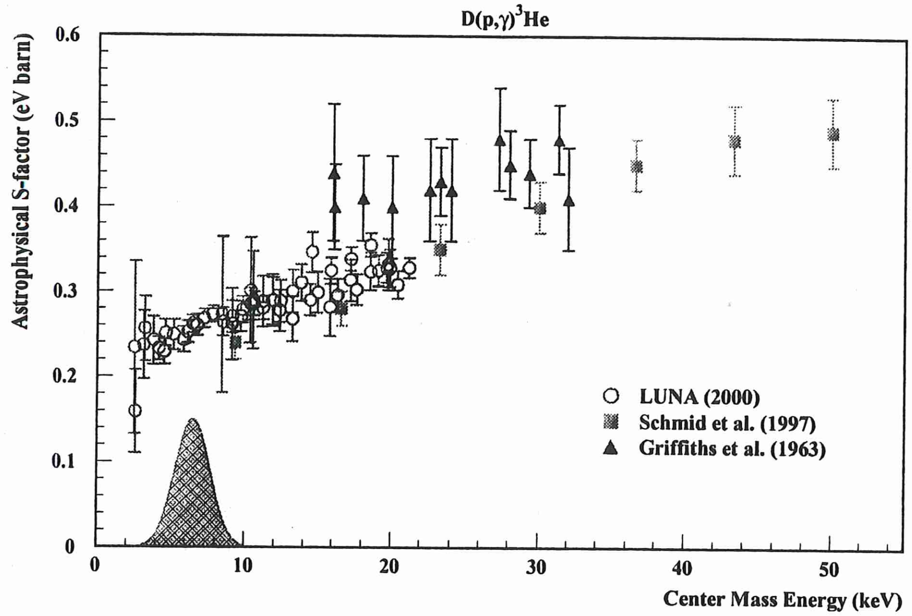

Figure 2: The D(p,γ)^{3}He astrophysical factor $S(E)$. The position of the solar Gamow peak is also shown schematically.

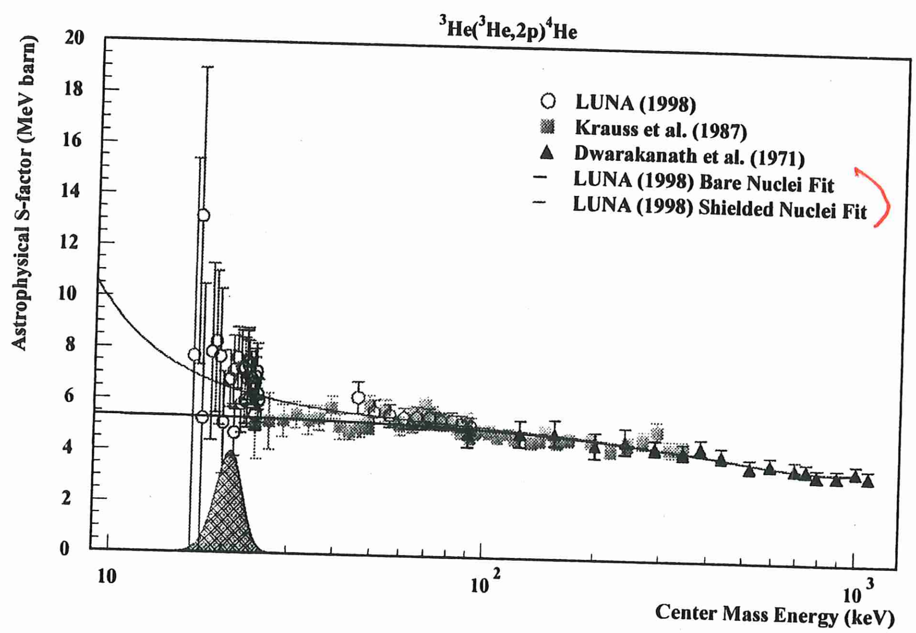

Figure 1: The $^3He(^3He,2p)^4He$ astrophysical factor $S(E)$. The position of the Gamow peak is also shown schematically.

SUMMARY

$$\langle \sigma v \rangle = \sqrt{\frac{8}{\pi \mu (kT)^3}} \int_0^\infty E\,\sigma(E)\, e^{-E/kT}\, dE$$

write

$$\sigma(E) = \frac{S(E)}{E}\, e^{-\sqrt{E_G/E}}$$

$$E_G = 2\mu e^2 (\pi Z_1 Z_2 \alpha)^2$$ GAMOW ENERGY

note $\alpha = e^2/\hbar c$

EXAMPLE

$^7Be(p,\gamma)^8B$ part of pp-chain

- No measurements below 111 keV after 50 yrs of experiments
- Solar Gamow window between 9 and 36 keV
- $\sigma(111)/\sigma(36) > 4500$!

∴ S(E) critical as is theory to constrain/define the form of S(E)

SCREENING

• LABORATORY (Cauldrons pp 165–168)

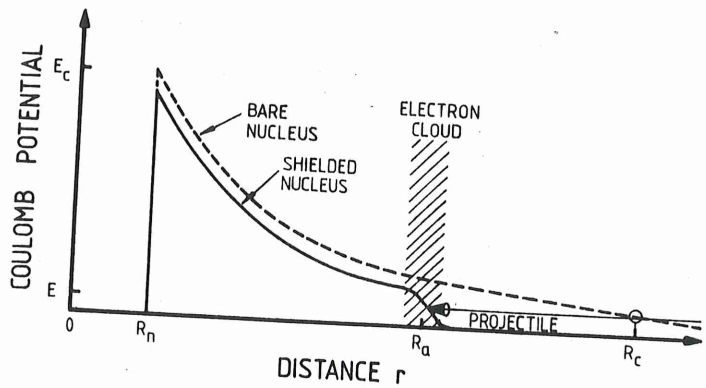

FIGURE 4.8. Shown in an exaggerated and idealized way is the effect of the atomic electron cloud on the Coulomb potential of a bare nucleus. This potential is reduced at all distances and goes essentially to zero beyond the atomic radius R_a. The effect of this electron shielding on an incident projectile is to increase the penetrability through the barrier, and thus also the cross section.

Note the shielded nucleus potential is narrower ∴ Tunneling probability is enhanced.

Typical case: Accelerated ion is stripped but target has atomic electrons

• Screening leads to $\langle\sigma v\rangle_{\text{screened}} > \langle\sigma v\rangle_{\text{bare nuclei}}$ at low energies

• Empirically corrected

$$\frac{\sigma_{sc}(E)}{\sigma_b(E)} = \frac{S_s(E)}{S_b(E)}\left(\frac{E}{E+U_e}\right)\exp\left(\pi\eta\,\frac{U_e}{E}\right)$$

$^3He(d,p)^4He$ ($Q = 18.4$ MeV) (LUNA expt)

$U_e = 219$ eV but might expect adiabatic limit ($\simeq$ diff. in electron binding energies between colliding atoms and the compound atom) $\simeq 120$ eV — Aliotta Fig 4, 5

$d(^3He,p)^4He$ [same reaction effectively]

$U_e = 109$ eV — expected $U_e = 65$ eV

same S(E) have at low E. but

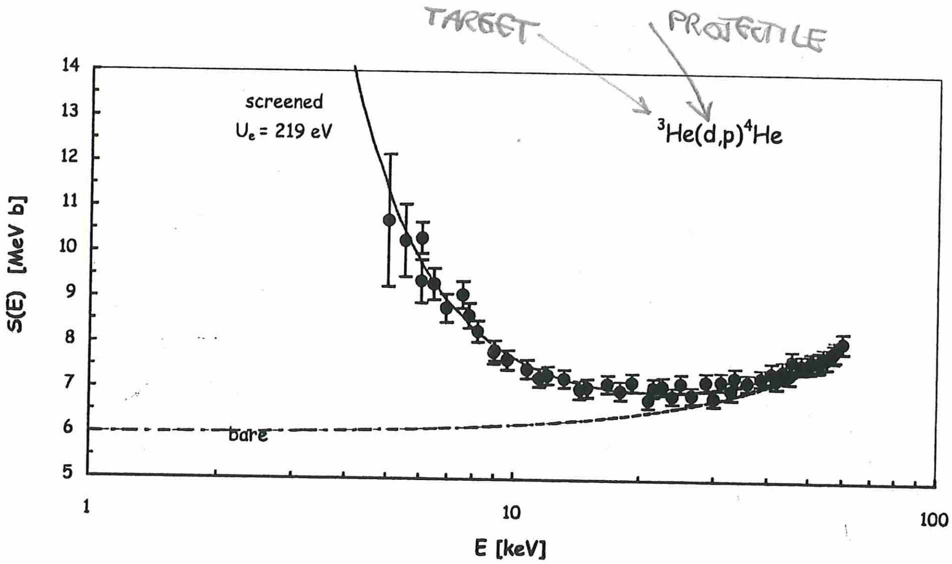

Fig. 4. $S(E)$ factor data for the ^{3}He(d, p)^{4}He reaction from the present work. The errors shown represent only statistical and accidental uncertainties, which were used in the fits. The dashed curve represents the $S(E)$ factor for bare nuclei and the solid curve that for screened nuclei with $U_e = 219$ eV.

SAME REACTION!

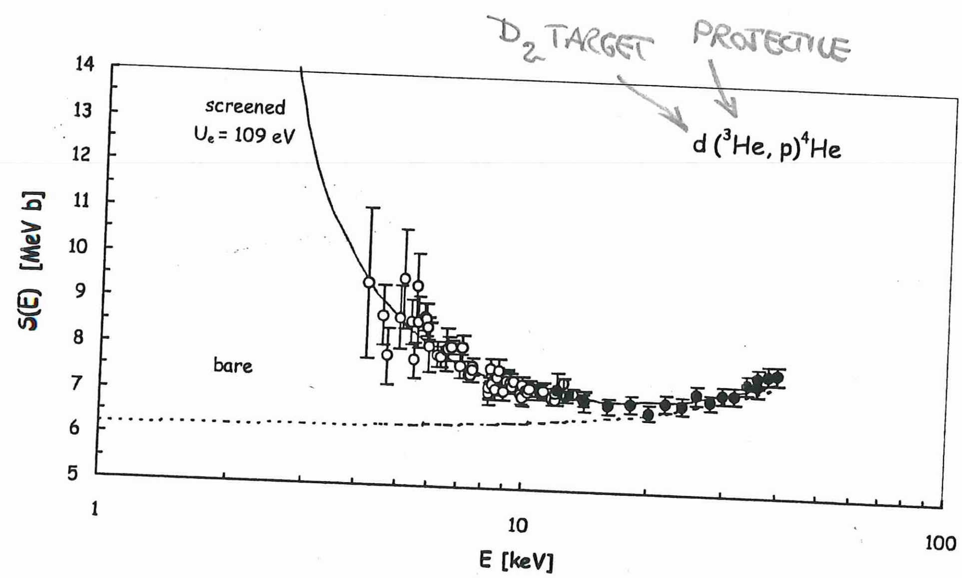

Fig. 5. $S(E)$ factor data for the d(^{3}He, p)^{4}He reaction from previous work [14] (open points) and present work (filled-in points), both obtained with the same LUNA setup. The errors shown represent only statistical and accidental uncertainties, which were used in the fits. The dashed curve represents the $S(E)$ factor for bare nuclei and the solid curve that for screened nuclei with $U_e = 109$ eV.

UPDATE – LATE NEWS

See Spitaleri et al. (astro-ph 1503.05266)

The electron screening puzzle and nuclear clustering

Accurate measurements of nuclear reactions of astrophysical interest within, or close to, the Gamow peak, show evidence of an unexpected effect attributed to the presence of atomic electrons in the target. The experiments need to include an effective "screening" potential to explain the enhancement of the cross sections at the lowest measurable energies. Despite various theoretical studies conducted over the past 20 years and numerous experimental measurements, a theory has not yet been found that can explain the cause of the exceedingly high values of the screening potential needed to explain the data. In this letter we show that instead of an atomic physics solution of the "electron screening puzzle", the reason for the large screening potential values is in fact due to clusterization effects in nuclear reactions, in particular for reaction involving light nuclei.

Nuclear clustering = $^6Li \equiv \alpha + d$, i.e., not a spherical nucleus.

- STELLAR INTERIORS

Free electrons screen nuclei
see Salpeter (1954)

$$f = \exp(-U_e/kT)$$
$$= \exp\left(\frac{Z_1 Z_2 e^2}{kTR_D}\right)$$

$$R_D = \left[kT/(4\pi e^2 \rho N_A \xi\right]^{1/2}$$

$$\xi = \sum_i (Z_i^2 + Z_i) \frac{X_i}{A_i}$$

Generally, $f \cong 1$ for non-degenerate gases